ERDC/CRREL TR-22-24

US Army Corps of Engineers®
Engineer Research and Development Center

ERDC ENGINEER RESEARCH & DEVELOPMENT CENTER

Army 6.1 Basic Research Program

A *k*-Means Analysis of the Voltage Response of a Soil-Based Microbial Fuel Cell to an Injected Military-Relevant Compound (Urea)

Robert M. Jones, Molly Creagar, Michael Musty, Randall Reynolds, Scott Michael Slone, and Robyn Barbato

November 2022

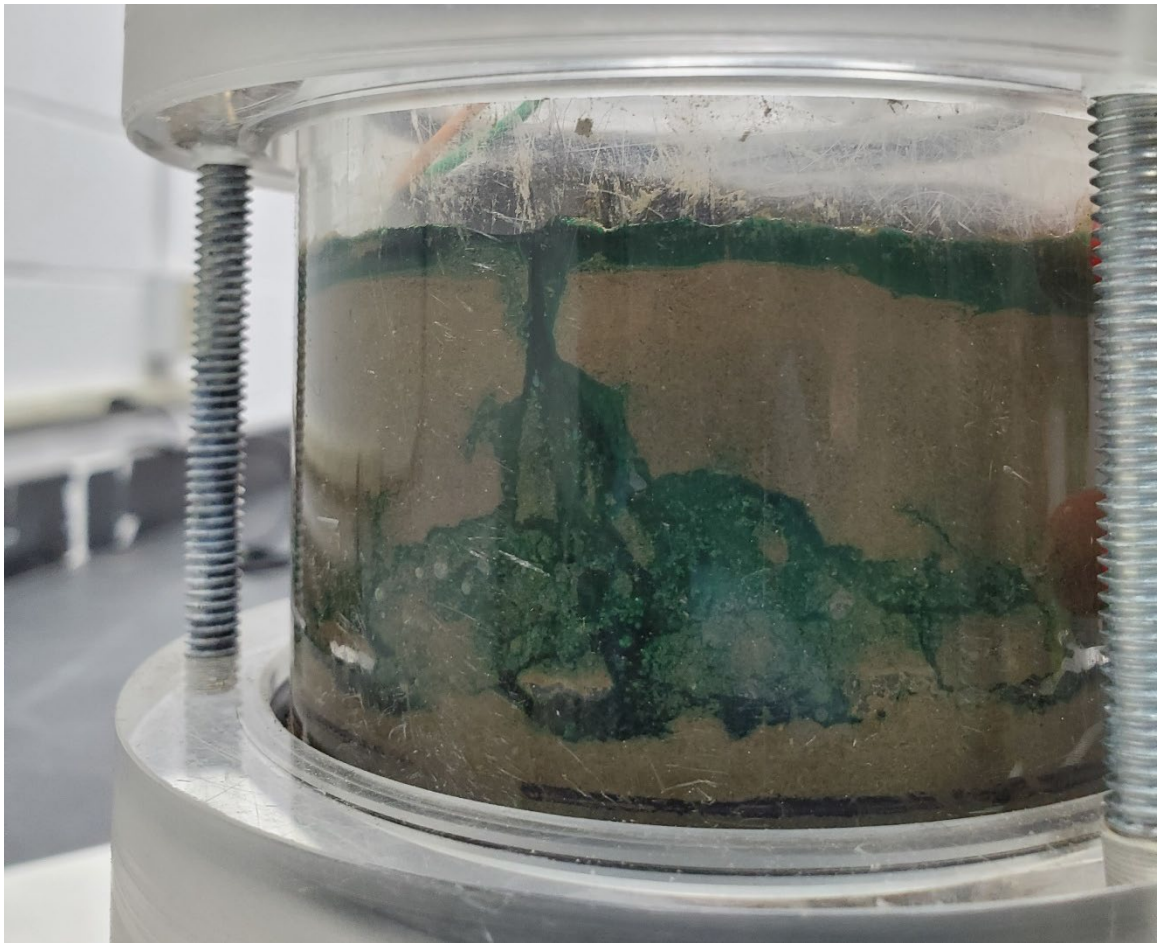

Cold Regions Research and Engineering Laboratory

The US Army Engineer Research and Development Center (ERDC) solves the nation's toughest engineering and environmental challenges. ERDC develops innovative solutions in civil and military engineering, geospatial sciences, water resources, and environmental sciences for the Army, the Department of Defense, civilian agencies, and our nation's public good. Find out more at www.erdc.usace.army.mil.

To search for other technical reports published by ERDC, visit the ERDC online library at https://erdclibrary.on.worldcat.org/discovery.

ERDC/CRREL TR-22-24
November 2022

A *k-Means* Analysis of the Voltage Response of a Soil-Based Microbial Fuel Cell to an Injected Military-Relevant Compound (Urea)

Robert M. Jones, Michael Musty, Randall Reynolds, Scott Michael Slone, and Robyn Barbato

U.S. Army Engineer Research and Development Center (ERDC)
Cold Regions Research and Engineering Laboratory (CRREL)
72 Lyme Road
Hanover, NH 03755-1290

Molly Creagar

The University of Nebraska Lincoln
College of Arts and Sciences, Department of Mathematics
Lincoln, NE 68588

Final Technical Report (TR)

Prepared for Headquarters, US Army Corps of Engineers
Washington, DC 20314-1000

Under PE 060102A, Project AB2, Task SAB202

Abstract

Biotechnology offers new ways to use biological processes as environmental sensors. For example, in soil microbial fuel cells (MFCs), soil electrogenic microorganisms are recruited to electrodes embedded in soil and produce electricity (measured by voltage) through the breakdown of substrate. Because the voltage produced by the electrogenic microbes is a function of their environment, we hypothesize that the voltage may change in a characteristic manner given environmental disturbances, such as the contamination by exogenous material, in a way that can be modelled and serve as a diagnostic. In this study, we aimed to statistically analyze voltage from soil MFCs injected with urea as a proxy for gross contamination. Specifically, we used *k*-means clustering to discern between voltage output before and after the injection of urea. Our results showed that the *k*-means algorithm recognized 4–6 distinctive voltage regions, defining unique periods of the MFC voltage that clearly identify pre- and postinjection and other phases of the MFC lifecycle. This demonstrates that *k*-means can identify voltage patterns temporally, which could be further improve the sensing capabilities of MFCs by identifying specific regions of dissimilarity in voltage, indicating changes in the environment.

Contents

Figures and Tables

Figures

Preface

This study was conducted Headquarters, US Army Corps of Engineers, under PE 060102A, Project AB2, Task SAB202.

The work was performed by the Biogeochemical Sciences Branch (Mr. Nathan J. Lamie, chief) and the Engineering Resources Branch (Dr. Melisa Nallar, acting chief) of the Research and Engineering Division, US Army Engineer Research and Development Center, Cold Regions Research and Engineering Laboratory (ERDC-CRREL). At the time of publication, Dr. Caitlin A. Callaghan was division chief. The acting deputy director of ERDC-CRREL was Mr. Bryan E. Baker, and the director was Dr. Joseph L. Corriveau.

COL Christian Patterson was commander of ERDC, and Dr. David W. Pittman was the director.

This page intentionally left blank.

1 Introduction

1.1 Background

1.1.1 Microbial fuel cells

In microbial fuel cells (MFCs), chemical energy can be converted to electrical energy through the metabolism of electrogenic, or electron-producing, microorganisms (Kim et al. 2007), allowing for the production of electricity through biological processes. Cultures of electrogenic organisms can be configured analogous to a traditional battery (i.e., composed of an electron-producing chamber filled with electrogenic microorganisms [anode] and an electron-consuming chamber [cathode]). The difference in electrical potential between the chambers promotes the flow of electrical current and thus power.

Found ubiquitously in nature (Chabert et al. 2015), electrogenic microorganisms have specialized metabolic pathways (Ishii et al. 2015; Aiyer 2020) and physical structures (Aiyer 2020) that enable them to create and relocate free electrons from various substrates. The well-studied electrogenic microorganism *Geobacter sulfurreducens*, for example, can use iron to reduce compounds and uses its conductive pili to transfer the resultant electrons to conductive surfaces, such as electrodes (Feliciano et al. 2015). In addition to iron, other electron acceptors of electrogenic microorganisms include nitrate, copper, and persulfate (Ucar et al. 2017). Additionally, the three main modes of electron transfer to the electrode include conductive pili, c-type cytochromes, and mediator molecules (Busalmen et al. 2008; Feliciano et al. 2015; Aiyer 2020).

As the electrogenic organisms predominantly favor low-oxygen environments, which electrochemically support the use of alternative electron acceptors (Chen et al. 2013), media such as sea sediment (Hong et al. 2010; Sajana et al. 2017) and wastewater (Liu et al. 2004; Munoz-Cupa et al. 2021) are commonly used in the construction of microbial fuel cells, with voltage outputs ranging from 300 to 800 mV* (Velasquez-Orta et al. 2011; Bose et al. 2018). However, there are also many electrogenic organisms

* For a full list of the spelled-out forms of the units of measure used in this document and their conversions, please refer to *US Government Publishing Office Style Manual*, 31st ed. (Washington, DC: US Government Publishing Office, 2016), 245–252 and 345–347, https://www.govinfo.gov/content/pkg/GPO-STYLEMANUAL-2016/pdf/GPO-STYLEMANUAL-2016.pdf.

found in terrestrial media as well, allowing for the operation of soil- and plant-based MFCs (Abbas and Rafatullah 2021; Maddalwar et al. 2021). The voltage output of these, though, is typically lower, ranging from 100 to 400 mV, largely because of the high resistivity of soils (Wolińska et al. 2014). However, while they may not possess the large influx of nutrients and organic matter that aids in producing sustainable power in wastewater-based MFCs (Liu et al. 2004), soil-based MFCs may have great utility in localized low-energy needs, such as the operation of lights that require minimal energy (Ieropoulos et al. 2016) and sensors for dissolved oxygen (Donovan et al. 2008; Shen et al. 2013). The dominant focus on the sustainable energy possibilities of MFCs has overshadowed that the MFC itself is a living microcosm that is responding to the environment and can therefore serve as a tool for observing environmental changes. Soil MFCs specifically are attractive candidates for terrestrial sensing because of their response to the addition of external substrates (Barbato et al. 2021)

1.1.2 Microbial fuel cells for change detection

The microorganisms in MFCs respond to changes in their environment. For instance, low temperatures slow the production of power in soil microbial fuel cells (Barbato et al. 2017). And while wastewater MFCs are good power generators overall, they must be kept at consistent conditions (e.g., temperature, pH, and dissolved oxygen), otherwise the power production can vary drastically (Marassi et al. 2019). Like any other microbial system, the energy produced, representative of the electrogenic microbial activity, depends on environmental parameters such as temperature, moisture, pH, and available nutrients. While changes in any of these parameters can be used to optimize microbial activity, the disturbance caused by fluctuations could also be utilized as a sensor for environmental change.

MFCs are sensitive to environmental perturbations (Liu et al. 2014; Jiang et al. 2018), such as changes in temperature, both static (Barbato et al. 2017) and oscillating (Dai et al. 2015; Liu et al. 2018; Gong et al. 2021), and influx of substrates (Liu et al. 2014; You et al. 2015; Do et al. 2020), and that sensitivity is reflected in their voltage patterns. For example, Dai et al. (2015) observed a close relationship to the increase and decrease of voltage-mirroring fluctuations in temperature and water level in rice paddy MFCs (i.e., voltage increased with increasing temperature and moisture and decreased with lower temperatures and moisture). MFCs could be particularly useful in detecting the introduction of substrates because different substrates may cause specific metabolic responses in

electrogenic microbes. It is possible that these metabolic responses could result in unique voltage changes that are characteristic of specific substrates. If this is the case, voltage data could be treated similarly to other time series data utilized to detect changes by using machine learning algorithms to understand what is "baseline" and what are "disturbed" voltages. From there, the algorithms can be trained to classify the disturbed voltage patterns based on the unique disturbance that caused them.

Prior research using soil MFCs for change detection has demonstrated that MFCs can measurably respond to the presence of a variety of compounds. For example, it has been observed that common carbon sources, fertilizer, NH_4^+, Mg^{2+}, and Fe^{2+}, each caused a change in voltage and current in MFCs (Adekunle et al. 2019). Another study demonstrated that the presence of five military-relevant compounds (i.e., gasoline; petroleum; 2,4-dinitrotoluene; fertilizer; and urea) resulted in statistically significant shifts in voltages from the control MFC (Barbato et al. 2021). Barbato et al (2021) demonstrated that *k*-means and radial-basis function-based machine learning algorithms could classify the compounds with more than a 90% average accuracy. However, a direct comparison between the voltage patterns of a soil-based MFC before and after the introduction of substrate has not been thoroughly explored.

This preliminary study introduced a nitrogen-based substrate, urea, to a stable soil-based MFC and continuously observed the voltage patterns. Urea was used because of its military relevance and significantly ($p < 0.0001$) elevated voltage output compared to the other military-relevant compounds tested in Barbato et al. (2021). The voltages were then clustered using a *k*-means pattern-recognition algorithm to identify specific regions and patterns of change that deviated significantly from the original stable voltage, allowing for the assessment of when and how the signal was disrupted by the introduction of substrate and if the voltage returned to preinjection values.

1.2 Objectives

MFCs have the potential to be dynamic sensors when exposed to the environment as the microbial activity of the electrogenic microbes (as measured by voltage) could be moved to characteristic voltage states by shifts in environmental conditions. For this study our primary interest was how the influx of an exogenous compound impacted the electrogenic microbial activity. Furthermore, this study hoped to capture the time-based dynamics

of the fuel cell after the perturbation by the exogenous compound to understand how the signal might change over time. To summarize these interests, we hypothesized that the addition of an exogenous compound, specifically urea, would cause a statistically significant voltage response identifiable through *k*-means clustering, enabling the differentiation between voltage produced before and after the exogenous compound was added to the MFCs. To test this hypothesis, we sought to accomplish the following objectives:

1. Measure voltage from soil MFCs after stabilization and then injection with urea.
2. Use *k*-means clustering to identify regions of change in the voltage patterns as a method of change detection caused by the introduction of substrate.

1.3 Approach

To accomplish the objectives, triplicate soil MFCs were constructed and had their voltage monitored continuously over 25 days. After 7 days, at which point the MFCs reached stability, 10 mL of a 2.16 mol/L urea solution was injected into the MFC from the bottom to create a 10.2 ppt urea area in the anode soil. After injection, the MFCs were operated for another 18 days before all data were collected. Data were analyzed with *k*-means clustering algorithms to identify regions of similar voltage to indicate distinctive regions of voltages. Clusters were then compared to microbial growth phenomena to describe the changes in voltage.

2 Methods

2.1 Fuel-cell chamber

2.1.1 Chamber construction

The microbial fuel-cell chamber was constructed from a 9.5 cm diameter plexiglass tube cut to a length of 8 cm with a thickness of 0.7 cm, resulting in a 412 cm^3 chamber. Caps for the tube were taken from 1405 Tempe Pressure Cells (Envco, Auckland, New Zealand) and were composed of plexiglass with an internal diameter of 8.2 cm. To seal the edges of the cap and the tube, a 0.5 cm O-ring was used. To create the injection port, a 1 cm diameter hole was drilled into the center of the bottom cap and a male-to-male tube port was wrapped in two layers of parafilm (Heathrow Scientific, Vernon Hills, Illinois, USA) and inserted through the hole. The port was sealed with a 0.2 cm thick septum and made airtight with epoxy. To create ports for the wires, two 0.5 cm diameter holes were drilled in the top of the chamber lid. Refer to Figure 1 for the chamber diagram.

Figure 1. Diagram of the microbial fuel-cell chambers before (*1*) and after construction with soil (*2*). Chambers were capped (*a*) with plexiglass and sealed with an O-ring (*b*). Cylindrical plexiglass makes the body of the chamber (*c*). A sealed port was inserted in the bottom cap to allow for injection (*d*). For construction, anode soil was placed in the bottom of the chamber (*e*), topped with a wired graphite felt (*f*), buried with cathode soil (*g*), and topped with a wired graphite felt (*h*). (Scale is approximate.)

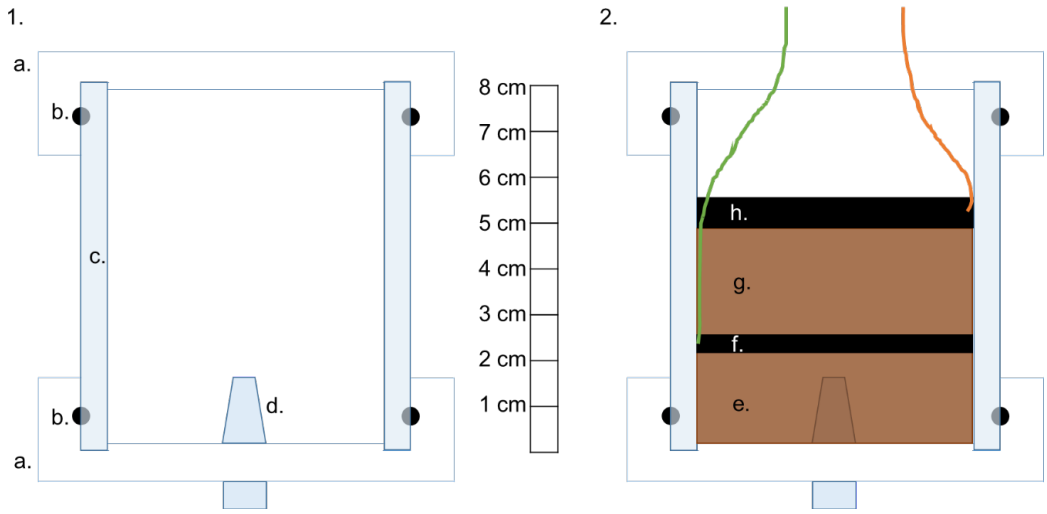

2.1.2 Chamber assembly

To construct the microbial fuel-cell microcosms, 1310 g of an air-dried sandy loam soil was first rehydrated with 360 mL of deionized water to 27% gravimetric water content, well mixed, and left covered and undisturbed at room temperature for 24 hr to allow microorganisms a chance to activate. In brief, the soil was composed of 66.6%–67.8% sand, 25.9%–26.7% silt, and 6.45%–6.49% clay; had a circumneutral pH; and was 3.3% organic matter (Barbato et al. 2015). Triplicate microcosm injection chambers (Figure 1) were each filled with approximately 155 g of wet soil taken from the bulk rehydrated material and tamped down manually until level to form an approximately 2 cm thick anode soil layer. A graphite felt (8 cm diameter, 0.5 cm thickness, Magical Microbes, College Station, Texas, USA) was pierced through the center with a titanium wire (Magical Microbes, College Station, Texas, USA) and placed on top of the anode soil layer in each chamber. In each chamber the anode felt was then buried with 230 g of wet soil taken from the bulk rehydrated material and manually tamped down until level to create an approximately 3 cm thick cathode soil layer. To serve as the cathode, a graphite felt (8.5 cm diameter, 1 cm thickness, Magical Microbes, College Station, Texas, USA) was pierced through the center with a titanium wire (Magical Microbes, College Station, Texas, USA) and placed on top of the cathode soil layer in each chamber. The greater thickness and area in the cathode are to allow more surface area for oxygen exchange to complete the cathodic reaction (Afsham et al. 2015). The wires were pulled through the ports of the lid for each chamber, and the ports were sealed with self-sticking labeling tape (Fisherbrand, Waltham, Massachusetts, USA) to reduce moisture loss. See Figure 1 for microcosm details. All replicate MFC microcosms were incubated at room temperature (approximately 25°C) under room lighting conditions (i.e., approximately 8 hours of synthetic light and 16 hours of darkness).

2.2 Voltage monitoring

To acquire voltage data for the MFCs, each set of wires was stripped of its insulation for 0.5 cm and crimped to an aluminum male connector (Adafruit, New York City, New York, USA). The male ends were inserted into aluminum female end adapters (Adafruit, New York City, New York, USA) and wired to a central I2C multiplexer (Adafruit, New York City, New York, USA). The multiplexer then sent signals to an ADS1115 (Adafruit, New York City, New York, USA), which converted them to analog signals

that were then passed to an Arduino Mega 2560 Rev3 microcontroller (Arduino LLC, Somerville, Massachusetts, USA). Voltage measurements were captured every 5 min and stored on an SD card inserted into the SD shield, except for brief periods when the Arduino was shut off to transfer data from the SD card. Figure 2 shows a diagram of the Arduino data acquisition system. The code for the operation of the Arduino can be found in the Appendix.

Figure 2. Arduino data acquisition system layout. An Arduino Mega microcontroller runs commands through the multiplexer to an analog-to-digital converter board wired to the three replicate MFCs. Data are stored on an SD card shield on the Arduino Mega.

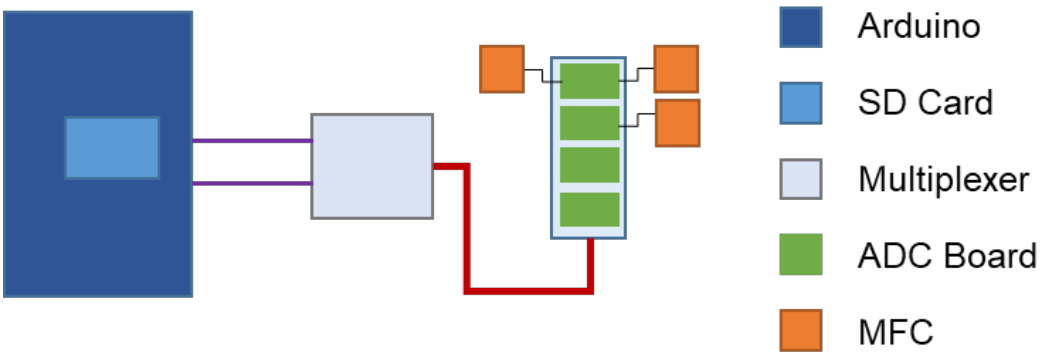

2.3 Injection

After construction, the MFCs were allowed to operate undisturbed for 7 days under the conditions described in Section 2.1.2. The 7-day period was to allow time for the MFC to produce electricity and reach a point of relative stability as noted by the decrease in slope (Figure 5). On day 7, 10 mL of a 2.16 mol/L solution of urea (Bio-Rad, Hercules, California, USA) in deionized water was injected through the bottom port of the chamber using a sterile 10 mL syringe and 22-gauge needle (BD, Franklin Lakes, New Jersey, USA). This concentration was chosen to achieve 10.2 ppt urea in the anode soil, which was the concentration tested in previous research demonstrating that urea had a statistical impact on the voltage output (Barbato et al. 2021). The syringe was inserted through the septum up to the syringe head, which positioned the end of the needle approximately 5 mm below the anode felt. The urea solution was manually injected into each microcosm at a rate of approximately 10 mL/min. The MFCs were then left undisturbed for another 18 days under the conditions described in Section 2.1.2 until stable voltage was achieved (Figure 5), resulting in a total of 25 days of operation. At the end of this period, all voltage data were transferred from the SD card to a computer for analysis,

resulting in over 7,000 points per microcosm. Data were also averaged across the three replicates and the standard error calculated. To assess the periods of stability, slopes for the voltage output were calculated for each 12 hr period (144 data points) using the slope function in R version 4.0.3 (R Core Team 2019).

2.4 *k*-means clustering

Data read from the Arduino was measured in milliseconds since activation and were converted to days since activation for all data points. Once converted, voltages were plotted using the ggplot package (Wickham 2016) in R version 4.0.3 (R Core Team 2019). To identify clusters of voltages, the data were imported into a Jupyter notebook running Python 3.8; the notebook code was modelled after the source code found in Xu (2020). The data were first cleaned of outliers using a rolling median approach, which removed data points found outside of three standard deviations in a window of five consecutive points. To reduce dimensionality, a principal components analysis was then performed on the cleaned data to find the top three principal components. These components aim to describe new characteristics not explicitly encoded in information in the data. In this particular study, the code and data were structured to try to encapsulate the changes in slope (consecutive point variability) and data characteristics within the principal components. From there, *k*-means clustering was used to calculate the error of each cluster from $k = 1, \ldots, 20$ clusters. The sum of squares error was plotted by number of clusters (Figure 3); and the elbow method (Kodinariya and Makwana 2013) was used to determine the optimal number of clusters, which appeared to be either 4, 5, or 6 clusters. These cluster groupings are considered optimal because they produce a low error and do not overfit the data (i.e., too many clusters can arbitrarily subdivide real clusters into false clusters whereas too few would not capture the true clusters and erroneously group different clusters). The data were then rerun using *k*-means and the three principal components identified previously to form clusters when the cluster numbers were 4, 5, and 6 independently. Once clusters were identified, they were plotted and colored by cluster (Figure 6*a*–*c*).

Figure 3. The sum of squares error by number of projected *k*-means cluster. As the number of clusters increases, typically the error decreases to near zero but can represent overfitting. Three *dashed lines* indicate the cluster sizes, 4 (*red*), 5 (*green*), 6 (*blue*) that are optimal in that they have low error but do not unnecessarily overfit the data.

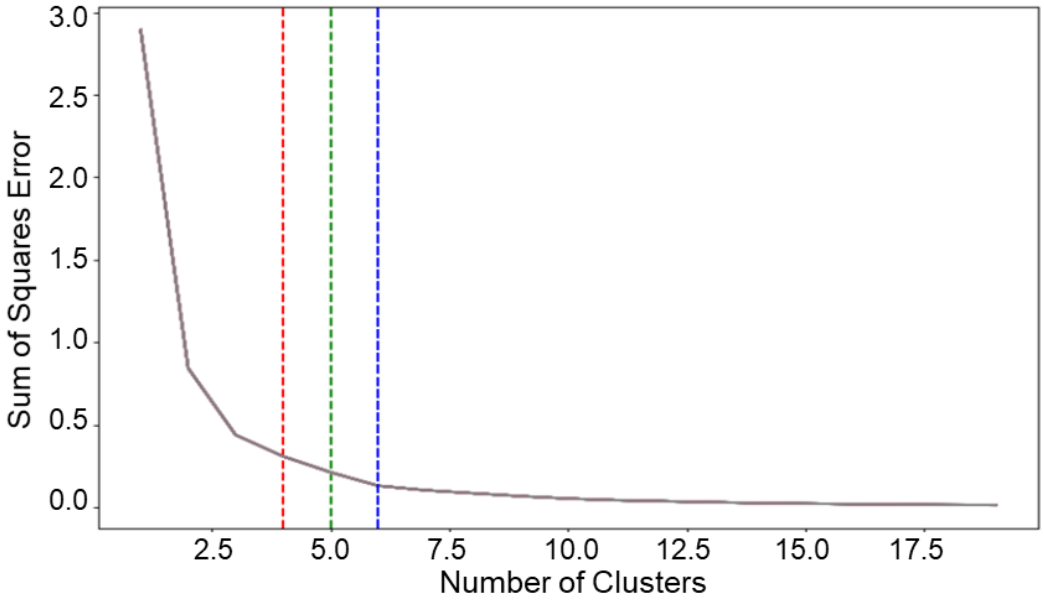

3 Results and Discussion

3.1 Voltage patterns through time

The primary objective of this study was to test if a pattern-recognition method such as *k*-means could identify which points in the voltage output of a microbial fuel cell deviated from previous stabilized output. In the case of the injection MFCs, we theorized this could correspond to pre- and postinjection voltages or, in the context of sensing, pre- and postdisturbance. The *k*-means algorithm was theorized to make an effective evaluator of when the voltage deviated from the norm as the algorithm specializes in recognizing when data points are part of the same series or source. In understanding the properties of each cluster, though, *k*-means could also indicate when the voltage returned to a previous range, such as the MFC reaching stable voltage after the initial perturbation. This would be signified by those periods being assigned the same cluster. Overall, any regions or points that are assigned the same cluster signify that the patterns are statistically similar whereas regions assigned different clusters are statistically dissimilar.

3.1.1 Voltage over time: preinjection

Figure 4*a* displays the first 6 days of the microbial-fuel-cell operation for the three replicate MFCs and is considered to be *preinjection*. For all replicates, it took approximately 1.5 days of operation before the voltage began to ramp upwards drastically, gaining over 500 mV between day 1.5 and 3 (Figure 4*d*; Figure 5). The sudden increase in voltage after a lag period is characteristic of the initial stages of MFC development (Read et al. 2010). Prior to the voltage increase, the replicates averaged 25 mV across the first 1.5 days (Figure 4*d* illustrates the average voltages and standard error across the replicates). In the next day, the replicate fuel cells substantially increased in voltage from an average of 72 mV to 410 mV. This trend of rapid increase continued until day 3 (Figure 5) when the voltages began to level out around 710 mV, suggesting the fuel cell was reaching a stable voltage and electrogenic activity (Read et al. 2010). From day 4 to day 6 and just before injection, the average voltage increased minimally (Figure 5) to a maximum average voltage of 812 mV.

Figure 4. Voltage output of replicate MFCs overtime. Voltage output for the first 6 days (*a*), voltage output up to and past the injection point (*b*), voltage output over the full 25-day period (*c*), and average voltage with standard error over the full 25-day period (*d*). The *dotted line* indicates the point of injection in all plots.

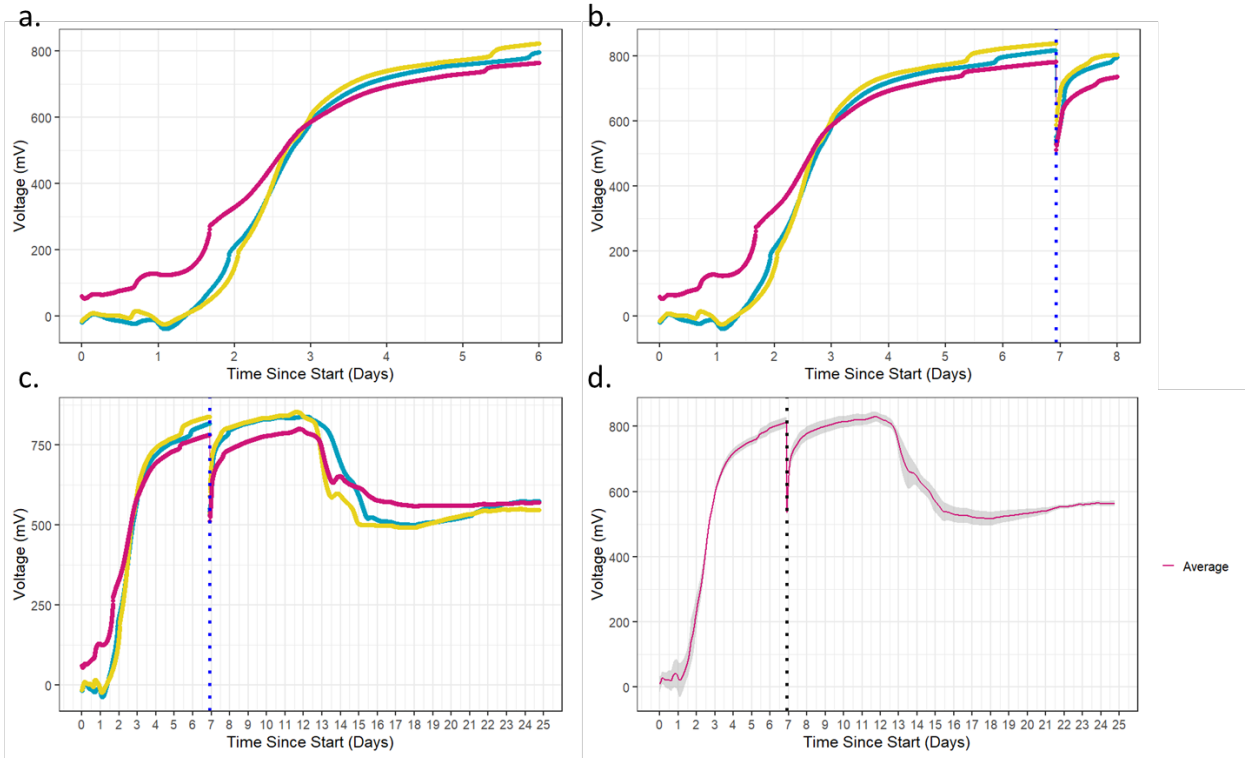

Figure 5. Slopes of average voltage taken every 12 hr (144 data points).

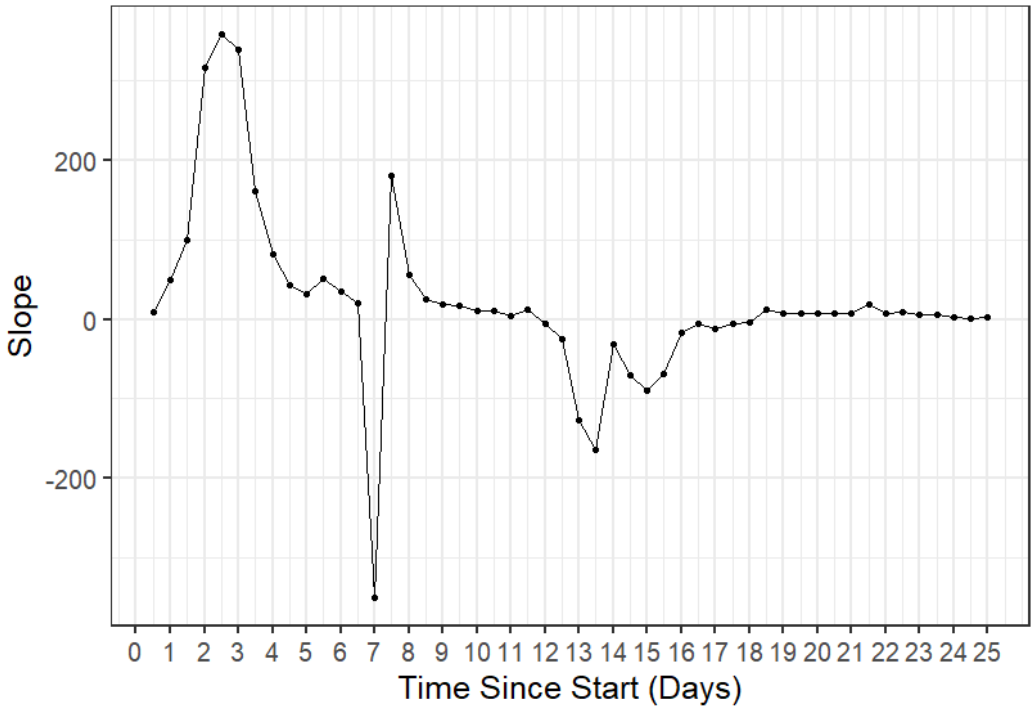

3.1.2 Voltage over time: injection and postinjection

Figure 4*b* displays the period just before and after the fuel cells were injected with urea (a period between day 0 and day 8). There was a clear drop in voltage at the point of injection, where each replicate decreased to just over 500 mV. However, within the next 24 hr, the fuel cells steadily climbed in voltage to an average of 778 mV by day 8. As the injection point was only a few millimeters from the anode surface, it is possible that the initial drop in voltage occurred due to physical and or chemical disruption of the biofilm at the anode surface or the soil around the surface of the anode. Indeed, as other microbial fuel cell studies have demonstrated, the voltage response to injected compounds can be almost immediate though variable, depending on the distance of the anode to port and the media injected (Mehta et al. 2010; Mardanpour et al. 2013; Liu et al. 2014). Furthermore, the abiotic influence of the urea was not directly measured. The period of recovery, therefore, could represent the relatively quick reestablishment of the disrupted biofilm or simply the fuel cell returning to electrochemical stability (Katuri and Scott 2011). It is worth noting also that, while small in concentration and predominantly localized to the anode, the presence of the urea solution may have changed the conductivity of the fuel cell and voltage (Simeon et al. 2019; Abbas and Rafatullah 2021). While it is possible that the influence of urea conductivity is relatively low in comparison to the impact to the microbial electrochemical reactions as demonstrated in Wang et al. (2017), more research is necessary to separate the changes in voltage caused chemically from those caused microbially as voltage shifts could be dependent on active community members and their metabolic processes (Karthikeyan et al. 2016).

On day 12, 5 days after the injection of urea, the average voltage value returned to the maxima range observed before injection 800–820 mV (Figure 4*d*). Interestingly, around day 13, all replicates began to rapidly decrease in voltage, dropping from an average 740 mV to 560 mV in a 48 hr period (Figure 4*d*). The rapid decline in voltage could be due to moisture loss as show in Habibul et al. (2016). However, this is not likely because the period immediately after day 15 shows the replicate fuel cells levelling out in voltage and even slightly increasing, holding at an average of 510 mV from day 16 to 18 (Figure 4*d*). From day 18 to 25, the replicate MFCs held a consistent voltage at an average of 560 mV (Figure 4*c*; Figure 5).

Without an accompanying microbial analysis of the anode community, it would be impossible to be certain, but the sudden decrease then

stabilization of voltage from day 13 to 15 suggests that the nature of the electroactive biofilm may have changed. It is possible that as the urea was further utilized and diffused through the soil closest to the anode and that microbes with greater affinity for nitrogen became increasingly active. As studies have demonstrated that urea is a ubiquitous nitrogen source for soil microorganisms (Hasan 2000), it is not unlikely that many community members could compete for the substrate and utilize it to their advantage. Alternatively, the redox reactions being used by the electrogenic microbes may have changed due to shifts in nutrient availability and redox states (Wang et al. 2018). Another possible explanation for the sudden decrease in voltage at day 13 is a shift in the biofilm strategy. For example, Kim and Lee (2016) observed that when some biofilms sense an abundance of nutrients, they disperse into a planktonic state, perhaps to take advantage of the rich environment. While this behavior has not been specifically linked to electroactive soil bacteria, it is possible that in the influx of urea at the later stages of the anode biofilm triggered a dispersal event, thus reducing the overall biofilm mass and potentially changing resource allocation from electroactivity to dispersal, hence an overall decrease in voltage.

3.2 *k*-means clustering of data points

A sum of squares error for projected *k*-means clustering determined that 4, 5, or 6 independent clusters would be appropriate cluster groupings to model the voltage data as they show convergence with the real number of clusters but do not overfit the data (Figure 3). In the context of this analysis, the *k*-means clustering treats every voltage point as an independent value regardless of time and looks for points of similar values or trajectories to isolate events or regions of similar output. In other words, time as a variable is removed and all points are analyzed as if they occur simultaneously, thus allowing the *k*-means algorithm to cluster points based solely on their voltage and how close that voltage is to other points. Thus, if points that were measured at the beginning of the study and points measured at the end have similar voltage, they can be appropriately clustered together though they are separated temporarily. Basing the clustering on voltage without the time component therefore can potentially identify when voltages have returned to a previous state. In looking at the various cluster series (Figure 6*a*–*c*), there are several distinctive events that denote unique voltage regions and correspond to the life cycle of the microbial fuel cell and occurrence of physical events that mirror the bacterial growth curve (Zwietering et al. 1990). These include the lag phase, or acclimation phase;

the exponential phase, or ascending phase; the stationary phase; and the declining phase (Li et al. 2008; Rodrigo et al. 2009; Sudarsan et al. 2015).

Figure 6. Visualization of *k*-means clustering of the average voltage over the 25-day observation period when 4 (*a*), 5 (*b*), and 6 (*c*) cluster groupings were used.

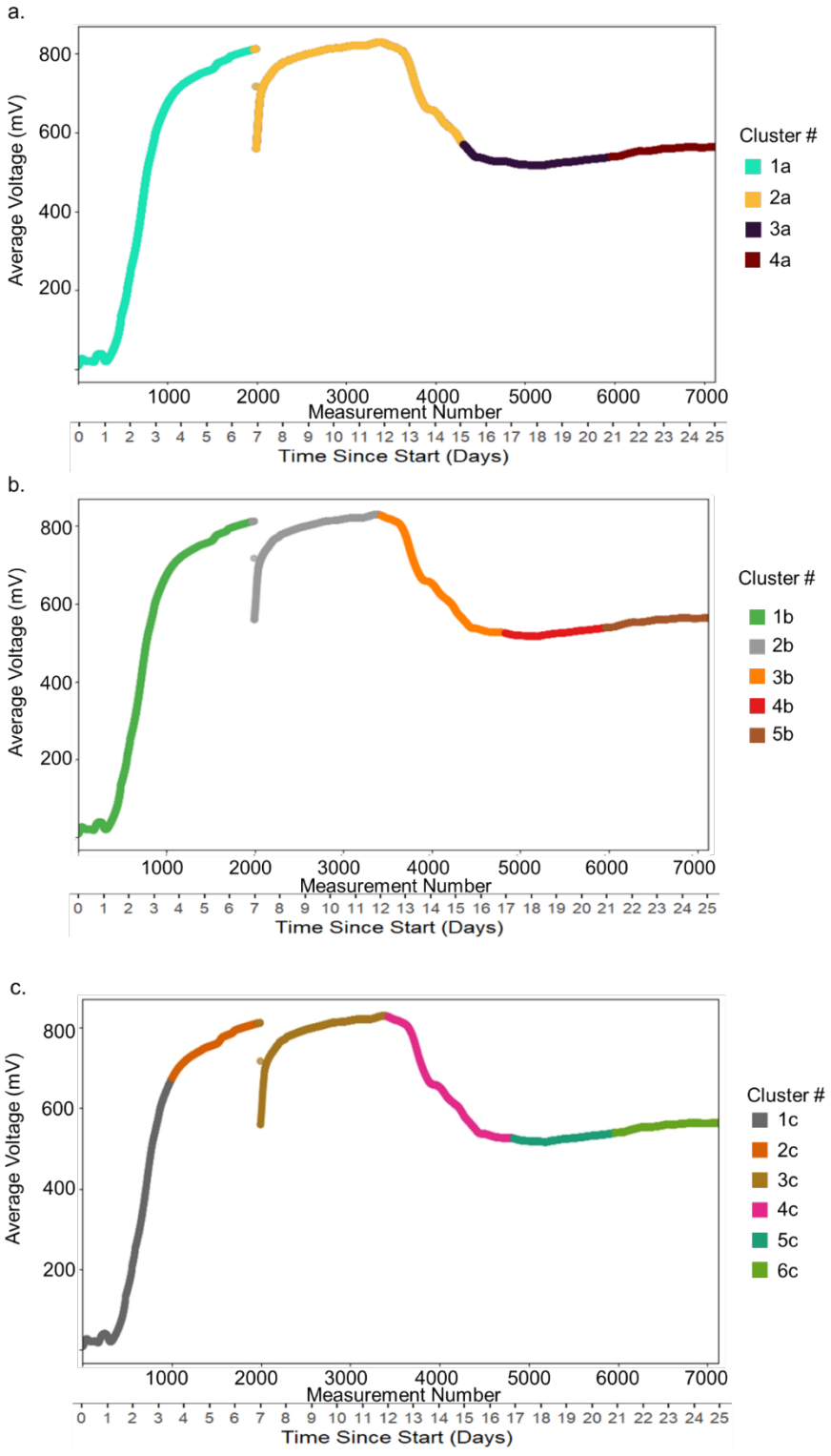

The four-cluster plot (Figure 6*a*) illustrates the least resolved clustering of the MFC voltage patterns; however, it identifies major voltage regions distinctly. Cluster 1a (Figure 6*a*) treats the period prior to injection as one event, including both the voltage ramp-up (acclimation and ascending phases) and the stabilization period from day 0 to 6. The *k*-means algorithm then recognizes the period of injection and the 5 days afterward, including the slow decline in voltage, as another region (Figure 6*a*, Cluster 2a). Note that though the voltage postinjection between points 2000 and 3200 (corresponding to days 7–12) returns to preinjection values of approximately 800 mV, the *k*-means algorithm does not recognize them as the same cluster. As the voltage ceases to decline and levels off for a stable period around point 4000, a new event is classified (Figure 6*a*, Cluster 3a), representing a new average voltage. Curiously, though the increase in voltage from point 6000 onwards (corresponding to days 20–25) is minimal (less than 10 mV) in comparison to more drastic increases and decreases (greater than 200 mV) witnessed earlier, such as the ascending phase (500–1500, days 1.5–4; Figure 5), the algorithm denotes the second stability point as its own event (Figure 6*a*, Cluster 4a).

To relate the results of the four-cluster plot to possible microbiological phenomena, we propose that Cluster 1a represents the inoculation of soil bacteria on the anode and cathode, biofilm formation, and voltage production; Cluster 2a represents the immediate decline of voltage from the disturbance from the injection, rapid increase, stabilization, and decline in voltage; Cluster 3a represents a stabilization period; and Cluster 4a represents continued stabilization (Li et al. 2008; Rodrigo et al. 2009; Sudarsan et al. 2014). It is clear that Cluster 2 should be separated further into more phases that represent visual changes in the voltage. This is not surprising, though, as the four-cluster grouping was toward the onset of the elbow (Figure 3), suggesting the possibility that more true clusters could be resolved. These regions and events become increasingly defined as the number of assigned clusters increases.

The most notable difference between the four-cluster (Figure 6*a*) and five-cluster (Figure 6*b*) outputs is the separation of the postinjection decline in voltage, points 3400–4800 (day 11.5–17), as its own event (Figure 6*b*, Cluster 3b). This seems appropriate as it is a markedly large decline (from 800 mV to 500 mV) in comparison to the relative stability of the voltage immediately prior to the decline, points 2500–3400 (days 9–11.5), which has also been designated as its own cluster (Figure 6*b*, Cluster 2b). It is

interesting to note that this decline occurs almost 4 days postinjection, which begs the question of what corresponding physical or chemical changes with the MFC are causing the sudden decline since it is separated temporarily from the initial injection and does not seem to be directly associated with the injection. If the decline was influenced by purely the presence of the urea, we might expect the decline in voltage to occur gradually as the urea diffuses throughout the system (Wang et al. 2013; Sirinutsomboon 2014). However, in the case of Cluster 3b, the decline occurs rapidly (–160 mV/12 hr; Figure 5) over 3 days. This suggests that the driving force behind the decrease in voltage was due to large changes in the anodic microbes (Zhang et al 2011).

An additional analysis that might aid in understanding the impact of the presence of urea would be a suite of MFCs injected only with deionized water. Still, without a more-thorough analysis, it would be impossible to determine whether these changes are due to shifts in microbial community members, change in biofilm integrity, or overall changes in microbe behavior. For future experiments, including uninjected control MFCs along with a microbial analysis could help uncover the specific shifts in microbial communities that correspond to changes in voltage. One potential theory to explain the voltage drop, however, is that with the influx of nutrients, which have diffused to the anode region, the electroactive biofilm may have shifted tactics and morphology to favor dispersion. While not observed ubiquitously in biofilm-forming microbes, there is evidence that nutrient flux can trigger dispersion events in some biofilms, particularly in the late stages (Kim and Lee 2016). If the electroactive biofilm is continuing to disperse and altering its metabolism to accommodate, this could explain the sudden decrease in voltage and the delay of this event as it may have taken a certain amount of time for the urea to aggregate around the anode in sufficient quantities to trigger dispersion. Following this theory, the reestablishment of voltage stability could indicate the end of this dispersion event and the shift of the biofilm back to a more static regulatory phase, or possibly additional colonization of microbes that took advantage of the abundance of nutrients and co-colonized the biofilm surface. Further studies and techniques, such as electrochemical impedance spectroscopy coupled with microbial community analysis, could help elucidate some of the biofilm dynamics of this period (He and Mansfield 2009).

Lastly and not surprisingly, the six-cluster analysis resulted in the highest number of clusters and demarcation of key changes in the voltage output

(Figure 6*c*). The six-cluster grouping is the only classification scheme that separates the ramp-up period (Figure 6*c*, Cluster 1c) and the preinjection stabilization period (Figure 6*c*, Cluster 2c) from one another, treating them as distinctive events. With the isolation of the ramp-up period, the six-cluster classification presents six events in the voltage patterns that possibly relate to electrogenic microbiological phenomena in the fuel cell. We theorize that Clusters 1c and 2c (Figure 6*c*) correspond to an initial colonization (acclimation phase) and rapid increase in voltage (ascending phase; Li et al. 2008; Rodrigo et al. 2009) followed by a period of relatively stable voltage (stationary phase) as the anodic community becomes established as is characteristic of microbial fuel cells (Logan et al. 2006; Read et al. 2010; Yanuka-Golub et al. 2016). Cluster 3c potentially illustrates the immediate disturbance to the biofilm from the physical influx of material and chemical shock of differing conditions (Mardanpour et al. 2013; Ghasemi Naraghi et al. 2015) but also the restabilization of the biofilm as suggested by the return to postinjection voltages. As was discussed previously with Cluster 3b (Figure 6*b*), Cluster 4c may represent a shift of the biofilm to a predominantly dispersed state, hence the decline in voltage, though it is also possible that the change in conditions around the anode encouraged competition among the other microbial communities that disrupted the voltages. The average voltage from Cluster 5c and 6c was 524 mV and 564 mV, respectively, which are only 7.4% different (Figure 6*c*). Even though there was a relatively small increase in voltage between Clusters 5c and 6c, they were denoted as distinct. This may be because the variance in voltages in these regions was minimal (48.6 and 58.8 respectively) in comparison to other clusters, thus creating dense centroids in the *k*-means clustering process (i.e., the points are too densely packed around their centroids to be treated as the same cluster). And to relate Clusters 5c and 6c (Figure 6*c*) to the electrogenic microbial community life stages, these two clusters potentially demonstrate a period in which the community returns to a stable point and a new voltage equilibrium is reached.

Regardless of the number of clusters, the *k*-means algorithm successfully distinguished voltage regions prior to and after injection as being distinctive. While the interpretation of the events the clusters represented in the MFCs needs further study and resolution, it is clear that the algorithm is able to distinguish between events involving rapid change (both positive and negative) and different levels of stability. However, this study examined a single induced change. It is unknown how this statistical analysis will apply to multiple increases and decreases in voltage from changing

environmental conditions that in situ MFCs might experience. For instance, periods of wetting and drying (Saeed and Miah 2021) or diurnal temperature cycles (Gong et al. 2021) could result in changes to microbial activity and in turn voltage output. While the source code example for this *k*-means method demonstrates the ability to identify cycles (Xu 2020), it is over a larger time, and it is unknown whether this could be replicated on a short timescale (hours) in which MFCs may experience large voltage changes. Despite that gap, however, it is clear that the *k*-means clustering algorithm is capable of detecting changes in the voltage patterns of the MFCs and identifying distinctive events at least in regard to the sudden introduction of substrate.

4 Conclusions

In this study, we measured the electrogenic microbial activity (voltage) of a soil-based MFC as it was exposed to an exogenous compound and demonstrated that the injection caused distinctive shifts in voltage. Through the *k*-means analysis of the voltage patterns using 4, 5, and 6 independent cluster groupings, it is also clear that there are several voltage states that occur throughout the lifetime of the MFC pre- and postinjection. While not covered in this study, the voltage states could be indicative of distinctive microbial behavior at the electrode surfaces, such as colonization, biofilm formation, and transition to planktonic state. However, further research would be necessary to validate that theory. To support this theory and better understand the MFC community, our future works will include an in-depth analysis of the microbial community through DNA sequencing and will address such questions as the community pre- and postinjection, shifts in community abundance correlated with voltage events, and active electrogenic community members.

This study also demonstrates that the MFC's response to the influx of an exogenous compound can be immediate, or at least observable on the order of minutes. The relatively high reaction speed of the MFC to the perturbations of the experiment further supports the use of MFCs as a sensor for change detection. Note, though, that this study performed "gross contamination" by applying a large amount of exogenous material, and more research would be necessary to determine the sensitivity of the MFC to minor perturbations.

While we cannot conclude from this study alone that any introduction of exogenous compounds will elicit an observable voltage response, the data do suggest that the *k*-means pattern-recognition algorithm has the resolution to identify minor and major changes in voltage states. Furthermore, the preinjection data also illustrates the potential utility of the *k*-means algorithm to aid in defining the natural stages of the MFC microbial community. This could be useful in building a strong model of what the "natural trajectory" for a soil-based MFC is to provide a basis for comparison when suspected perturbations have occurred.

A crucial further point of study would be to incorporate other environmental factors known to have a strong influence on microbial activity. Factors such as moisture and temperature can be deterministic of microbial

growth and activity and could also have an impact on the voltage output of the electrogenic microbial community, perhaps even overshadowing or exacerbating the response caused by exogenous compounds. Additionally, injection controls such as injecting deionized water could improve our understanding of how much of the voltage response is due to disturbance versus the chemical nature of the compound. Similarly, control MFCs that do not experience injection could be valuable in understanding what a normal undisturbed voltage pattern looks like and, when coupled with a microbial community analysis, could highlight which community members change most when compared to MFCs that experience injection.

Given the possible sensitivities to environmental variables, the next logical step is also to compare the effectiveness of the *k*-means algorithm on MFC voltages that have been deployed in the field. Field MFCs will likely experience inconsistent changes in temperature, moisture, and nutrient introduction that could be challenging for the *k*-means algorithm to capture but would aid in building a strong dynamic model for using the voltages to inform on the environment. However, as the data in this study suggests, *k*-means may be capable of identifying changes in the steady state of the MFC voltage regardless of the cause; and more study would be necessary to parse the shifts in voltage into categories, such as shifts due to natural effects versus anthropogenic effects.

When the variables (environmental and physical) are more resolved, the *k*-means analysis could feed into a larger model that seeks to sense and characterize contamination in situ. Artificial intelligence chips, for instance, have the capability to resolve complex patterns through machine learning when trained with sufficient data. In the context of MFCs, the data in question could be voltage patterns of MFCs impacted by a variety of contaminants, each one potentially having a unique voltage pattern. This could have applications in both security, by detecting and classifying illicit compounds or compounds indicative of human activity when MFCs are deployed in restricted areas, or in environmental monitoring, by detecting environmental contaminants in a range of concentrations. The *k*-means analysis of voltage patterns when MFCs are field deployed can help train the model in understanding what is a normal voltage pattern and what is a voltage pattern impacted by a disturbance, thus potentially allowing the model to make highly resolved judgements and utilize the data effectively. For example, the *k*-means algorithm might be able to identify periods of voltage that cluster with natural variation and identify periods of voltage

that are anomalous to the rest of the voltage history and thus necessitating further resolution by the machine learning algorithm. To make this application feasible, more research is needed on how the voltage patterns respond to the dynamic nature of environments they might be deployed in and how pattern recognition and machine learning algorithms interpret these potentially dynamic voltage patterns. If *k*-means and machine learning algorithms are able to work in concert and resolve the complex voltage patterns of MFCs, it could allow for the use of MFCs as low-input sensors for contaminant detection in the environment.

References

Abbas, Syed Zaghum, and Mohd Rafatullah. 2021. "Recent Advances in Soil Microbial Fuel Cells for Soil Contaminants Remediation." *Chemosphere* 272:129691. https://doi.org/10.1016/j.chemosphere.2021.129691.

Adekunle, Ademola, Vijaya Raghavan, and Boris Tartakovsky. 2019. "A Comparison of Microbial Fuel Cell and Microbial Electrolysis Cell Biosensors for Real-Time Environmental Monitoring." *Bioelectrochemistry* 126:105–112. https://doi.org/10.1016/j.bioelechem.2018.11.007.

Adhikari, Ramesh Y., Nikhil S. Malvankar, Mark T. Tuominen, and Derek R. Lovley. 2016. "Conductivity of Individual *Geobacter* Pili." *RSC Advances* 6 (10): 8354–8357. https://doi.org/10.1039/C5RA28092C.

Afsham, N., R. Roshandel, S. Yaghmaei, V. Vajihinejad, and M. Sherafatmand. 2015. "Bioelectricity Generation in a Soil Microbial Fuel Cell with Biocathode Denitrification." *Energy Sources, Part A: Recovery, Utilization, and Environmental Effects* 37 (19): 2092–2098. https://doi.org/10.1080/15567036.2012.671900.

Aiyer, Kartik S. 2020. "How Does Electron Transfer Occur in Microbial Fuel Cells?" *World Journal of Microbiology and Biotechnology* 36 (2). https://doi.org/10.1007/s11274-020-2801-z.

Barbato, Robyn A., Robert M. Jones, Michael A. Musty, and Scott M. Slone. 2021. "Reading the Ground: Understanding the Response of Bioelectric Microbes to Anthropogenic Compounds in Soil Based Terrestrial Microbial Fuel Cells." *PLoS ONE* 16 (12): e0260528. https://doi.org/10.1371/journal.pone.0260528.

Barbato, Robyn A., Karen L. Foley, Jorge A. Toro-Zapata, Robert M. Jones, and Charles M. Reynolds. 2017. "The Power of Soil Microbes: Sustained Power Production in Terrestrial Microbial Fuel Cells under Various Temperature Regimes." *Applied Soil Ecology* 109: 14–22. https://doi.org/10.1016/j.apsoil.2016.10.001.

Barbato, Robyn A., Karen L. Foley, and Charles M. Reynolds. 2015. *Soil Temperature and Moisture Effects on Soil Respiration and Microbial Community Abundance*. ERDC/CRREL TR-15-6. Hanover, NH: Engineer Research and Development Center, Cold Regions Research and Engineering Laboratory.

Bose, Debajyoti, Himanshi Dhawan, Vaibhaw Kandpal, Parthasarthy Vijay, and Margavelu Gopinath. 2018. "Bioelectricity Generation from Sewage and Wastewater Treatment Using Two-Chambered Microbial Fuel Cell." *International Journal of Energy Research* 42 (14): 4335–4344. https://doi.org/10.1002/er.4172.

Busalmen, Juan P., Abraham Esteve-Núñez, Antonio Berná, and Juan Miguel Feliu. 2008. "C-Type Cytochromes Wire Electricity-Producing Bacteria to Electrodes." *Angewandte Chemie International Edition* 47 (26): 4874–4877. Wiley. https://doi.org/10.1002/anie.200801310.

Chabert, Nicolas, Oulfat Amin Ali, and Wafa Achouak. 2015. "All Ecosystems Potentially Host Electrogenic Bacteria." *Bioelectrochemistry* 106 (A): 88–96. https://doi.org/10.1016/j.bioelechem.2015.07.004.

Chen, Chih-Yu, Tzu-Yu Chen, and Ying-Chien Chung. 2013. "A Comparison of Bioelectricity in Microbial Fuel Cells with Aerobic and Anaerobic Anodes." *Environmental Technology* 35 (3): 286–293. https://doi.org/10.1080/09593330.2013.826254.

Dai, Jianing, Jun-Jian Wang, Alex T. Chow, and William H. Conner. 2015. "Electrical Energy Production from Forest Detritus in a Forested Wetland Using Microbial Fuel Cells." *GCB Bioenergy* 7 (2): 244–252. https://doi.org/10.1111/gcbb.12117.

Do, Minh Hang, Huu Hao Ngo, Wenshan Guo, Soon Woong Chang, Dinh Duc Nguyen, Yiwen Liu, Sunita Varjani, and Mathava Kumar. 2020. "Microbial Fuel Cell-Based Biosensor for Online Monitoring Wastewater Quality: A Critical Review." *Science of The Total Environment* 712:135612. https://doi.org/10.1016/j.scitotenv.2019.135612.

Donovan, Conrad, Alim Dewan, Deukhyoun Heo, and Haluk Beyenal. 2008. "Batteryless, Wireless Sensor Powered by a Sediment Microbial Fuel Cell." *Environmental Science and Technology* 42 (22):8591–8596. https://doi.org/10.1021/es801763g.

Feliciano, G. T., R. J. Steidl, and G. Reguera. 2015. "Structural and Functional Insights into the Conductive Pili of *Geobacter Sulfurreducens* Revealed in Molecular Dynamics Simulations." *Physical Chemistry Chemical Physics* 17 (34): 22217–22226. https://doi.org/10.1039/c5cp03432a.

Ghasemi Naraghi, Zahra, Soheila Yaghmaei, Mohammad Mahdi Mardanpour, and Masoud Hasany. 2015. "Produced Water Treatment with Simultaneous Bioenergy Production Using Novel Bioelectrochemical Systems." *Electrochimica Acta* 180:535–544. https://doi.org/10.1016/j.electacta.2015.08.136.

Gong, Lingling, Mehran Abbaszadeh Amirdehi, Amine Miled, and Jesse Greener. 2021. "Practical Increases in Power Output from Soil-Based Microbial Fuel Cells under Dynamic Temperature Variations." *Sustainable Energy and Fuels* 5 (3): 671–677. https://doi.org/10.1039/d0se01406k.

Habibul, Nuzahat, Yi Hu, and Guo-Ping Sheng. 2016. "Microbial Fuel Cell Driving Electrokinetic Remediation of Toxic Metal Contaminated Soils." *Journal of Hazardous Materials* 318 (15): 9–14. https://doi.org/10.1016/j.jhazmat.2016.06.041.

Hasan, H. A. H. 2000. "Ureolytic Microorganisms and Soil Fertility: A Review." *Communications in Soil Science and Plant Analysis* 31 (15–16): 2565–2589. https://doi.org/10.1080/00103620009370609.

He, Zhen, and Florian Mansfeld. 2009. "Exploring the Use of Electrochemical Impedance Spectroscopy (EIS) in Microbial Fuel Cell Studies." *Energy and Environmental Science* 2 (2): 215–219. https://doi.org/10.1039/b814914c.

Hong, Seok Won, Han S. Kim, and Tai Hak Chung. 2010. "Alteration of Sediment Organic Matter in Sediment Microbial Fuel Cells." *Environmental Pollution* 158 (1): 185–191. https://doi.org/10.1016/j.envpol.2009.07.022.

Ieropoulos, Ioannis Andrea, Andrew Stinchcombe, Iwona Gajda, Samuel Forbes, Irene Merino-Jimenez, Grzegorz Pasternak, Daniel Sanchez-Herranz, and John Greenman. 2016. "Pee Power Urinal—Microbial Fuel Cell Technology Field Trials in the Context of Sanitation." *Environmental Science: Water Research and Technology* 2 (2): 336–343. https://doi.org/10.1039/c5ew00270b.

Ishii, Shun'ichi, Shino Suzuki, Aaron Tenney, Trina M. Norden-Krichmar, Kenneth H. Nealson, and Orianna Bretschger. 2015. "Microbial Metabolic Networks in a Complex Electrogenic Biofilm Recovered from a Stimulus-Induced Metatranscriptomics Approach." *Scientific Reports* 5 (1): 14840. https://doi.org/10.1038/srep14840.

Jiang, Yong, Xufei Yang, Peng Liang, Panpan Liu, and Xia Huang. 2018. "Microbial Fuel Cell Sensors for Water Quality Early Warning Systems: Fundamentals, Signal Resolution, Optimization and Future Challenges." *Renewable and Sustainable Energy Reviews* 81 (1): 292–305. https://doi.org/10.1016/j.rser.2017.06.099.

Karthikeyan, Rengasamy, Ammayaippan Selvam, Ka Yu Cheng, and Jonathan Woon-Chung Wong. 2016. "Influence of Ionic Conductivity in Bioelectricity Production from Saline Domestic Sewage Sludge in Microbial Fuel Cells." *Bioresource Technology* 200: 845–852. https://doi.org/10.1016/j.biortech.2015.10.101.

Katuri, Krishna P., and Keith Scott. 2011. "On the Dynamic Response of the Anode in Microbial Fuel Cells." *Enzyme and Microbial Technology* 48 (4–5): 351–358. https://doi.org/10.1016/j.enzmictec.2010.12.011.

Kim, Byung Hong, In Seop Chang, and Geoffrey M. Gadd. 2007. "Challenges in Microbial Fuel Cell Development and Operation." *Applied Microbiology and Biotechnology* 76 (3): 485–494. https://doi.org/10.1007/s00253-007-1027-4.

Kim, Soo-Kyoung, and Joon-Hee Lee. 2016. "Biofilm Dispersion in Pseudomonas Aeruginosa." *Journal of Microbiology* 54 (2): 71–85. https://doi.org/10.1007/s12275-016-5528-7.

Kodinariya, Trupti M., and Prashant R. Makwana. 2013. "Review on Determining Number of Cluster in K-Means Clustering." *International Journal* 1 (6): 90–95.

Li, Zhenglong, Lu Yao, Lingcai Kong, and Hong Liu. 2008. "Electricity Generation Using a Baffled Microbial Fuel Cell Convenient for Stacking." *Bioresource Technology* 99 (6): 1650–1655. https://doi.org/10.1016/j.biortech.2007.04.003.

Liu, Bingchuan, Yu Lei, and Baikun Li. 2014. "A Batch-Mode Cube Microbial Fuel Cell Based 'Shock' Biosensor for Wastewater Quality Monitoring." *Biosensors and Bioelectronics* 62:308–314. https://doi.org/10.1016/j.bios.2014.06.051.

Liu, Boyue, Min Ji, and Hongyan Zhai. 2018. "Anodic Potentials, Electricity Generation and Bacterial Community as Affected by Plant Roots in Sediment Microbial Fuel Cell: Effects of Anode Locations." *Chemosphere* 209:739–747. https://doi.org/10.1016/j.chemosphere.2018.06.122.

Liu, Hong, Ramanathan Ramnarayanan, and Bruce E. Logan. 2004. "Production of Electricity during Wastewater Treatment Using a Single Chamber Microbial Fuel Cell." *Environmental Science and Technology* 38 (7): 2281–2285. https://doi.org/10.1021/es034923g.

Logan, Bruce E., Bert Hamelers, René Rozendal, Uwe Schröder, Jürg Keller, Stefano Freguia, Peter Aelterman, Willy Verstraete, and Korneel Rabaey. 2006. "Microbial Fuel Cells: Methodology and Technology." *Environmental Science and Technology* 40 (17):5181–5192. https://doi.org/10.1021/es0605016.

Maddalwar, Shrirang, Kush Kumar Nayak, Manish Kumar, and Lal Singh. 2021. "Plant Microbial Fuel Cell: Opportunities, Challenges, and Prospects." *Bioresource Technology* 341 (2021): 125772. https://doi.org/10.1016/j.biortech.2021.125772.

Marassi, R. J., R. S. Hermanny, G. C. Silva, F. T. Silva, and T. C. B. Paiva. 2019. "Electricity Production and Treatment of High-Strength Dairy Wastewater in a Microbial Fuel Cell Using Acclimated Electrogenic Consortium." *International Journal of Environmental Science and Technology* 16 (11): 7339–7348. https://doi.org/10.1007/s13762-019-02391-7.

Mardanpour, Mohammad Mahdi, Mohsen Nasr Esfahany, Tayebeh Behzad, Ramin Sedaqatvand, Forough Sharifi, and Fatemeh Naderi. 2013. "Factors Affecting the Performance of Single Chamber Microbial Fuel Cell Using a Novel Configuration." *Iranian Journal of Energy and Environment* 4(4): 343e7.

Mehta, P., A. Hussain, B. Tartakovsky, V. Neburchilov, V. Raghavan, H. Wang, and S. R. Guiot. 2010. "Electricity Generation from Carbon Monoxide in a Single Chamber Microbial Fuel Cell." *Enzyme and Microbial Technology* 46(6): 450–455. https://doi.org/10.1016/j.enzmictec.2010.02.010.

Munoz-Cupa, Carlos, Yulin Hu, Chunbao Xu, and Amarjeet Bassi. 2021. "An Overview of Microbial Fuel Cell Usage in Wastewater Treatment, Resource Recovery and Energy Production." *Science of The Total Environment* 754:142429. https://doi.org/10.1016/j.scitotenv.2020.142429.

R Core Team. 2019. R: A Language and Environment for Statistical Computing. Vienna, Austria: R Foundation for Statistical Computing. https://www.R-project.org/.

Read, Suzanne T., Paritam Dutta, Phillip L Bond, Jürg Keller, and Korneel Rabaey. 2010. "Initial Development and Structure of Biofilms on Microbial Fuel Cell Anodes." *BMC Microbiology* 10 (98). https://doi.org/10.1186/1471-2180-10-98.

Rodrigo, Manuel A., Pablo Cañizares, Hugo García, Jose J. Linares, and Justo Lobato. 2009. "Study of the Acclimation Stage and of the Effect of the Biodegradability on the Performance of a Microbial Fuel Cell." *Bioresource Technology* 100 (20): 4704–4710. https://doi.org/10.1016/j.biortech.2009.04.073.

Saeed, Tanveer, and Md Jihad Miah. 2021. "Organic Matter and Nutrient Removal in Tidal Flow-Based Microbial Fuel Cell Constructed Wetlands: Media and Flood-Dry Period Ratio." *Chemical Engineering Journal* 411:128507. https://doi.org/10.1016/j.cej.2021.128507.

Sajana, T. K., M. M. Ghangrekar, and A. Mitra. 2017. "In Situ Bioremediation Using Sediment Microbial Fuel Cell." *Journal of Hazardous, Toxic, and Radioactive Waste* 21 (2): 04016022. https://doi.org/10.1061/(asce)hz.2153-5515.0000339.

Shen, Yujia, Meng Wang, In Seop Chang, and How Yong Ng. 2013. "Effect of Shear Rate on the Response of Microbial Fuel Cell Toxicity Sensor to Cu(II)." *Bioresource Technology* 136 (2013): 707–710. https://doi.org/10.1016/j.biortech.2013.02.069.

Sirinutsomboon, Bunpot. 2014. "Modeling of a Membraneless Single-Chamber Microbial Fuel Cell with Molasses as an Energy Source." *International Journal of Energy and Environmental Engineering* 5:93. https://doi.org/10.1007/s40095-014-0093-5.

Simeon, Meshack Imologie, Martins Yusuf Otache, Temidayo Abayomi Ewemoje, and Abdulganiy Olayinka Raji. 2019. "Application of Urine as Fuel in a Soil-Based Membrane-Less Single Chamber Microbial Fuel Cell." *CIGR Journal* 21 (1): 115–121. https://cigrjournal.org/index.php/Ejounral/article/view/4808.

Sudarsan, J. S., K. Prasana, S. Nithiyanantham, and K. Renganathan. 2014. "Comparative Study of Electricity Production and Treatment of Different Wastewater Using Microbial Fuel Cell (MFC)." *Environmental Earth Sciences* 73 (5): 2409–2413. https://doi.org/10.1007/s12665-014-3590-1.

Ucar, Deniz, Yifeng Zhang, and Irini Angelidaki. 2017. "An Overview of Electron Acceptors in Microbial Fuel Cells." *Frontiers in Microbiology* 8:643. https://doi.org/10.3389/fmicb.2017.00643.

Velasquez-Orta, S. B., I. M. Head, T. P. Curtis, and K. Scott. 2011. "Factors Affecting Current Production in Microbial Fuel Cells Using Different Industrial Wastewaters." *Bioresource Technology* 102 (8): 5105–5112. https://doi.org/10.1016/j.biortech.2011.01.059.

Wang, Haiping, Sunny C. Jiang, Yun Wang, and Bo Xiao. 2013. "Substrate Removal and Electricity Generation in a Membrane-Less Microbial Fuel Cell for Biological Treatment of Wastewater." *Bioresource Technology* 138:109–116. https://doi.org/10.1016/j.biortech.2013.03.172.

Wang, Hui, Xian Cao, Lei Li, Zhou Fang, and Xianning Li. 2018. "Augmenting Atrazine and Hexachlorobenzene Degradation under Different Soil Redox Conditions in a Bioelectrochemistry System and an Analysis of the Relevant Microorganisms." *Ecotoxicology and Environmental Safety* 147:735–741. https://doi.org/10.1016/j.ecoenv.2017.09.033.

Wang, Luguang, Beizhen Xie, Ningshengjie Gao, Booki Min, and Hong Liu. 2017. "Urea Removal Coupled with Enhanced Electricity Generation in Single-Chambered Microbial Fuel Cells." *Environmental Science and Pollution Research* 24 (25): 20401–20408. https://doi.org/10.1007/s11356-017-9689-7.

Wickham, Hadley. 2016. "Data Analysis." In *ggplot2: Elegant Graphics for Data Analysis. Use R!* Springer International Publishing. https://doi.org/10.1007/978-3-319-24277-4_9.

Wolińska, Agnieszka, Zofia Stępniewska, Arletta Bielecka, and Jakub Ciepielski. 2014. "Bioelectricity Production from Soil Using Microbial Fuel Cells." *Applied Biochemistry and Biotechnology* 173 (8): 2287–2296. https://doi.org/10.1007/s12010-014-1034-8.

Xu, J, 2020. Time Series Pattern Recognition with Air Quality Sensor Data. Source code, commit e2d0aae. GitHub. https://github.com/zhouxu-ds/air-quality-pattern-recognition/blob/main/notebook/clustering.ipynb.

Yanuka-Golub, Keren, Leah Reshef, Judith Rishpon, and Uri Gophna. 2016. "Community Structure Dynamics during Startup in Microbial Fuel Cells—The Effect of Phosphate Concentrations." *Bioresource Technology* 212: 151–159. https://doi.org/10.1016/j.biortech.2016.04.016.

You, Jiseon, X. Alexis Walter, John Greenman, Chris Melhuish, and Ioannis Ieropoulos. 2015. "Stability and Reliability of Anodic Biofilms under Different Feedstock Conditions: Towards Microbial Fuel Cell Sensors." *Sensing and Bio-Sensing Research* 6: 43–50. https://doi.org/10.1016/j.sbsr.2015.11.007.

Zhang, Yifeng, Booki Min, Liping Huang, and Irini Angelidaki. 2011. "Electricity Generation and Microbial Community Response to Substrate Changes in Microbial Fuel Cell." *Bioresource Technology* 102 (2): 1166–1173. https://doi.org/10.1016/j.biortech.2010.09.044.

Zwietering, M. H., I. Jongenburger, F. M. Rombouts, and K. van 't Riet. 1990. "Modeling of the Bacterial Growth Curve." *Applied and Environmental Microbiology* 56 (6): 1875–1881. https://doi.org/10.1128/aem.56.6.1875-1881.1990.

Appendix: Arduino Code for Voltage Measurements

```
#include <SPI.h>
#include <SD.h>
#include <Wire.h>
#include <Adafruit_ADS1015.h>

#define TCAADDR       0x70
#define ADS1115_ADDR0 0x48
#define ADS1115_ADDR1 0x49
#define ADS1115_ADDR2 0x4A
#define ADS1115_ADDR3 0x4B
#define PAUSE_MS      300000
#define I2C_CHANNELS  5
#define ADS1115_NUM   4
#define LOG_STATUS    7

String filename = "datalog.csv";

// On the Ethernet Shield, CS is pin 4. Note that even if it's not
// used as the CS pin, the hardware CS pin (10 on most Arduino
boards,
// 53 on the Mega) must be left as an output or the SD library
// functions will not work.
const int chipSelect  = 4;

File dataFile;

// initialize all ADC
Adafruit_ADS1115 ads  = Adafruit_ADS1115(ADS1115_ADDR0);  /* Use
this for the 16-bit version */
Adafruit_ADS1115 ads1 = Adafruit_ADS1115(ADS1115_ADDR1);  /* Use
this for the 16-bit version */
Adafruit_ADS1115 ads2 = Adafruit_ADS1115(ADS1115_ADDR2);  /* Use
this for the 16-bit version */
Adafruit_ADS1115 ads3 = Adafruit_ADS1115(ADS1115_ADDR3);  /* Use
this for the 16-bit version */

float multiplier;// = 0.0625F; /* ADS1115  @ +/- 6.144V gain (16-
bit results) */

String line;// line to write to file

/*
 * Setup the arduino for data logging, and ADC measurement read-
ings
 */
void setup() {
  // Open serial communications and wait for port to open:
  Serial.begin(9600);
  setup_adc();
  setup_sd_output();
  write_header();// write the output file header
```

```
}

/*
 * select i2c channel on TCA board
 */
void tcaselect(uint8_t i)
{
  if (i > 7) return;//error check value

 // switch the I2C bus
  Wire.beginTransmission(TCAADDR);
  Wire.write(1 << i);
  Wire.endTransmission();
}

/*
 * setup the sd car output
 */
void setup_sd_output()
{
  Serial.print("Initializing SD card...");
  // make sure that the default chip select pin is set to
  // output, even if you don't use it:
  pinMode(SS, OUTPUT);

  // see if the card is present and can be initialized:
  if (!SD.begin(10,11,12,13)) {
    Serial.println("Card failed, or not present");
    // don't do anything more:
    while (1) ;
  }
  Serial.println("card initialized.");

  // Open up the file we're going to log to!
  dataFile = SD.open("datalog.csv", FILE_WRITE);
  if (! dataFile) {
    Serial.println("error opening " + filename);
    // Wait forever since we cant write data
    while (1) ;
  }

  // let the user know the file is logging
  pinMode(LOG_STATUS,OUTPUT);
  digitalWrite(LOG_STATUS,HIGH);
}

/*
 * setup the ads1115 adcs. all 4 per channel
 */
void setup_adc()
{
  //
ADS1015  ADS1115
  //
-------  -------
  // ads.setGain(GAIN_TWOTHIRDS);  // 2/3x gain +/- 6.144V  1 bit
= 3mV      0.1875mV (default)
```

```
  // ads.setGain(GAIN_ONE);        // 1x gain   +/- 4.096V  1 bit
= 2mV      0.125mV
  // ads.setGain(GAIN_TWO);        // 2x gain   +/- 2.048V  1 bit
= 1mV      0.0625mV
  // ads.setGain(GAIN_FOUR);       // 4x gain   +/- 1.024V  1 bit
= 0.5mV    0.03125mV
  // ads.setGain(GAIN_EIGHT);      // 8x gain   +/- 0.512V  1 bit
= 0.25mV   0.015625mV
  // ads.setGain(GAIN_SIXTEEN);    // 16x gain  +/- 0.256V  1 bit
= 0.125mV  0.0078125mV
  multiplier = 0.0625;// mV/LSB
  Serial.println("Getting differential reading from AIN0 (P) and
AIN1 (N)");
  Serial.print("ADC Range: +/- 6.144V (1 bit = ");
  Serial.print(multiplier,DEC);
  Serial.println("mV/ADS1115)");
  ads.setGain(GAIN_TWO);
  ads.begin();
  ads1.setGain(GAIN_TWO);
  ads1.begin();
  ads2.setGain(GAIN_TWO);
  ads2.begin();
  ads3.setGain(GAIN_TWO);
  ads3.begin();
}

/*
 * take measurements from 4 ADC boards and return
 */
void take_measurements()
{
  int16_t r1, r2, r3, r4, r5, r6, r7, r8;

  r1 = ads.readADC_Differential_0_1();
  r2 = ads.readADC_Differential_2_3();
  r3 = ads1.readADC_Differential_0_1();
  r4 = ads1.readADC_Differential_2_3();
  r5 = ads2.readADC_Differential_0_1();
  r6 = ads2.readADC_Differential_2_3();
  r7 = ads3.readADC_Differential_0_1();
  r8 = ads3.readADC_Differential_2_3();

  // concatenate all values in a string
  line += "," + String(r1 * multiplier) + "," + String(r2 * multi-
plier) + "," +
      String(r3 * multiplier) + "," + String(r4 * multiplier) +
"," +
      String(r5 * multiplier) + "," + String(r6 * multiplier) +
"," +
      String(r7 * multiplier) + "," + String(r8 * multiplier);
}

/*
 * writes the output file header
 */
void write_header()
{
```

```
  String header = "Time (ms)";
  for (int i = 0; i < I2C_CHANNELS; i++)
  {
    for (int j = 0; j < ADS1115_NUM; j++)// two devices
    {
      for (int k = 0; k < 2; k++)// two differnetial channels
      {
        header += ",I2C" + String(i) + " 0x" +
String(ADS1115_ADDR0+j,HEX) + " CH" + String(k) + " (mV)";
      }
    }
  }
  Serial.println(header);
  dataFile.println(header);
  dataFile.flush();// flsuh data to file
}

/*
 * write the measurements to the file
 */
void write_measurements()
{
  Serial.println(line);
  dataFile.println(line);

  // The following line will 'save' the file to the SD card after
every
  // line of data - this will use more power and slow down how
much data
  // you can read but it's safer!
  // If you want to speed up the system, remove the call to
flush() and it
  // will save the file only every 512 bytes - every time a sector
on the
  // SD card is filled with data.
  dataFile.flush();
}

/*
 * loop to continuously run
 */
void loop() {
  line = String(millis());// initialize the line with a timestamp

  // cycle through all 12c channels
  for (int i = 0; i < I2C_CHANNELS; i++)
  {
    tcaselect(i);// select the i2x channel
    take_measurements();// take measurements from that channel
  }

  // write all measurements to a file
  write_measurements();

  // Take 1 measurement every 500 milliseconds
  delay(PAUSE_MS);
}
```

REPORT DOCUMENTATION PAGE

Form Approved

OMB No. 0704-0188

1. REPORT DATE (DD-MM-YYYY)	2. REPORT TYPE	3. DATES COVERED (From - To)
November 2022	Final Technical Report (TR)	FY19–FY22

4. TITLE AND SUBTITLE

A k-Means Analysis of the Voltage Response of a Soil-Based Microbial Fuel Cell to an Injected Military-Relevant Compound (Urea)

5a. CONTRACT NUMBER

5b. GRANT NUMBER

5c. PROGRAM ELEMENT

060102A

6. AUTHOR(S)

Robert M. Jones, Molly Creagar, Michael Musty, Randall Reynolds, Scott Michael Slone, and Robyn Barbato

5d. PROJECT NUMBER

AB2

5e. TASK NUMBER

SAB202

5f. WORK UNIT NUMBER

7. PERFORMING ORGANIZATION NAME(S) AND ADDRESS(ES)

US Army Engineer Research and Development Center (ERDC)
Cold Regions Research and Engineering Laboratory (CRREL)
72 Lyme Road
Hanover, NH 03755-1290

The University of Nebraska Lincoln
College of Arts and Sciences,
Department of Mathematics
Lincoln, NE 68588

8. PERFORMING ORGANIZATION REPORT NUMBER

ERDC/CRREL TR-22-24

9. SPONSORING / MONITORING AGENCY NAME(S) AND ADDRESS(ES)

Headquarters, US Army Corps of Engineers
Washington, DC 20314-1000

10. SPONSOR/MONITOR'S ACRONYM(S)

USACE

11. SPONSOR/MONITOR'S REPORT NUMBER(S)

12. DISTRIBUTION / AVAILABILITY STATEMENT

Approved for public release; distribution is unlimited.

13. SUPPLEMENTARY NOTES

14. ABSTRACT

Biotechnology offers new ways to use biological processes as environmental sensors. For example, in soil microbial fuel cells (MFCs), soil electrogenic microorganisms are recruited to electrodes embedded in soil and produce electricity (measured by voltage) through the breakdown of substrate. Because the voltage produced by the electrogenic microbes is a function of their environment, we hypothesize that the voltage may change in a characteristic manner given environmental disturbances, such as the contamination by exogenous material, in a way that can be modelled and serve as a diagnostic. In this study, we aimed to statistically analyze voltage from soil MFCs injected with urea as a proxy for gross contamination. Specifically, we used *k*-means clustering to discern between voltage output before and after the injection of urea. Our results showed that the *k*-means algorithm recognized 4–6 distinctive voltage regions, defining unique periods of the MFC voltage that clearly identify pre- and postinjection and other phases of the MFC lifecycle. This demonstrates that *k*-means can identify voltage patterns temporally, which could be further improve the sensing capabilities of MFCs by identifying specific regions of dissimilarity in voltage, indicating changes in the environment.

15. SUBJECT TERMS

Biosensors, Biotechnology, Contaminant detection, k-means, Pattern recognition, Soil microbial fuel cells, Soil pollution--Detection, Soil sensors, Voltage patterns

16. SECURITY CLASSIFICATION OF:			17. LIMITATION OF ABSTRACT	18. NUMBER OF PAGES	19a. NAME OF RESPONSIBLE PERSON
a. REPORT	b. ABSTRACT	c. THIS PAGE			19b. TELEPHONE NUMBER (include area code)
Unclassified	Unclassified	Unclassified	SAR	40	